

Optical multicolor polarization observations in the region of the open cluster NGC 5749^{*,**}

M. M. Vergne^{***}, C. Feinstein^{***}, and R. Martínez

Facultad de Ciencias Astronómicas y Geofísicas, Observatorio Astronómico, Paseo del Bosque, 1900 La Plata, Argentina
 e-mail: cfeinstein@fcaglp.edu.ar
 Instituto de Astrofísica de La Plata, CONICET

Received 6 October 2004 / Accepted 21 September 2006

ABSTRACT

We present (*UBVRI*) multicolor linear polarimetric data for 31 of the brightest stars in the area of the open cluster NGC 5749 considered to study the properties of the interstellar medium (ISM) towards the cluster. Our data yield a mean polarization percentage of $P_V \sim 1.7\%$, close to the polarization value produced by the ISM with normal efficiency ($P(\%) = 3.5E_{(B-V)}^{0.8}$) for a mean color excess of $E_{B-V} = 0.42$. The mean angle of polarization vectors, $\theta = 74^\circ$, agrees quite well with the expected angle produced by dust particles aligned in the direction of the galactic disk (and the magnetic field) in the region. Our analysis indicates that the visual absorption affecting the stars in NGC 5749 is partially produced by a dust layer located up to 300 pc from the Sun and also by a second layer of dust closer to the cluster (located at least at 700 pc). The observed photometry and our polarization data are consistent with the existence of dust within the cluster. We also show in this work how polarimetry could be an excellent technique for identifying nonmember stars.

Key words. ISM: dust, extinction – open clusters and associations: individual: NGC 5749

1. Introduction

NGC 5749 (C1445-543) is a poorly populated open cluster with little central concentration located at $l = 319.5$ and $b = 4.5$, near the south-western edge of the Lupus constellation. Lynga (1964a,b) carried out a photometric study (in three colors) of 15 bright stars in the field of NGC 5749, deriving a color excess $E_{B-V} = 0.35$ and a distance of 0.9 kpc. The most thorough study published is by Clariá and Lapasset (1992, hereafter CL), who got photoelectric *UBV* data of 112 stars brighter than $V = 14.4$, located within about $15'$ from the assumed cluster center. Their color–color diagram suggests possible variable reddening among the cluster members with an average excess of $E_{B-V} = 0.42 \pm 0.04$, a distance of 1280 ± 118 pc, and an age of 2.7×10^7 yr.

Studies of interstellar polarization are important for two reasons: they provide information on the dust itself and a means to trace the galactic magnetic field. Comparison of polarization and extinction data in the same lines of the sight provides tests for models of extinction and alignment of the grains. As they are thought to align so that their longest axes tend to become orthogonal to the direction of the local magnetic field, the observed polarization vectors map the mean field direction projected on the plane of the sky. This allows us to investigate

the structure of both the macroscopic field in our Galaxy (Mathewson & Ford 1970; Axon & Ellis 1976) and the local field associated with the individual clouds (Goodman et al. 1990).

The polarimetric technique is a very useful tool to obtain significant information (magnetic field direction, λ_{\max} , P_{\max} , etc.) from the dust located in front of a luminous object. In particular, young open clusters are very good candidates to carry out polarimetric observations because previous photometric and spectroscopic studies of these clusters have provided detailed information on the color and luminosity of the main sequence stars of the cluster. Thus, we can compute the physical parameters of the clusters (age, distance, extinction, membership, etc.) and then, with the polarimetric data, we can study the location, size, and efficiency of the dust grains to polarize the starlight and the different directions of the galactic magnetic field in the line of sight to the cluster. As the open clusters are also spread within an area, the evolution of the physical parameters of the dust all over the region can be analyzed. Additionally, the polarimetry data can be used as a powerful criterion for determining the membership in a galactic cluster (e.g., Feinstein et al. 2003a) and for detecting the location of an energetic phenomenon that occurred in the history of a cluster (Feinstein et al. 2003b).

For some years now, we have been carrying out systematic polarimetric observations in a large number of galactic open clusters. The aim of this survey is to provide clues about the characteristics of the dust responsible for the extinction and polarization in the light from cluster members, about its spatial distribution, and also about possible memberships. Following our ongoing program, we have performed polarimetry in the open cluster NGC 5749. In this paper we report the results of the multicolor (*UBVRI*) measurements of polarization in NGC 5749. We studied the characteristics (P_{\max} , λ_{\max} , polarization efficiency, etc.) of the dust located along the line of sight towards the region

* Based on observations obtained at Complejo Astronómico El Leoncito (CASLEO), operated under agreement between the CONICET and the National Universities of La Plata, Córdoba, and San Juan, Argentina.

** Table 1 is only available in electronic form at the CDS via anonymous ftp to cdsarc.u-strasbg.fr (130.79.128.5) or via <http://cdsweb.u-strasbg.fr/cgi-bin/qcat?J/A+A/462/621>

*** Member of the Carrera del Investigador Científico, CONICET, Argentina.

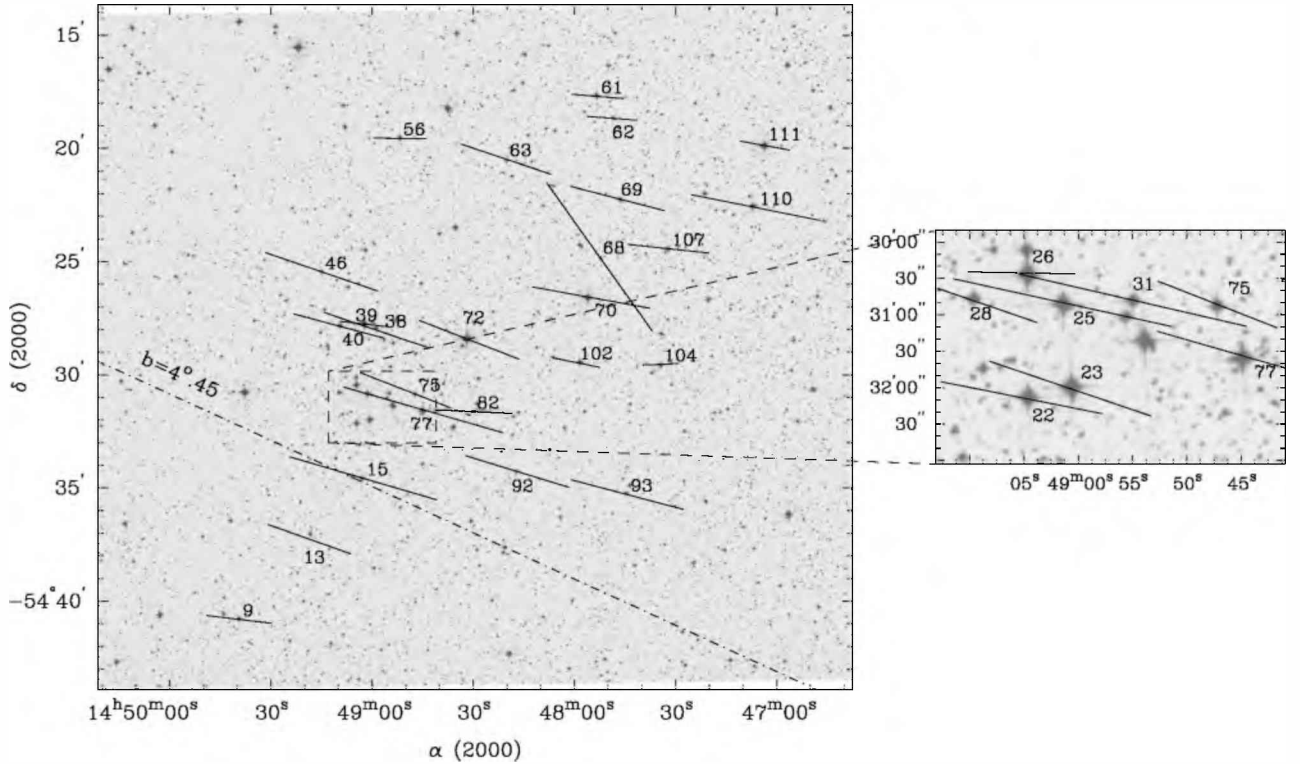


Fig. 1. Projection on the sky of the polarization vectors (Johnson V filter) of the stars observed in the region of NGC 5749. The dot-dashed line is the galactic parallel $b = 4.45$

where the cluster is situated. In the next sections, we will discuss the observations in the region, the data calibrations, and the results of both the individual stars and the cluster as a whole.

2. Observations and data reduction

Data on linear optical polarimetry were obtained during two observing runs at the Complejo Astronómico El Leoncito (CASLEO) in San Juan, Argentina, in 2003 (April 29 to May 5 and August 29 to September 2). The observations were carried out using the Torino five-channel photopolarimeter (Scaltriti 1994) attached to the 2.15-m telescope. Each star was observed simultaneously through the Johnson-Cousins broad band *UBVRI* filters ($\lambda_{U\text{eff}} = 0.360 \mu\text{m}$, $\lambda_{B\text{eff}} = 0.440 \mu\text{m}$, $\lambda_{V\text{eff}} = 0.530 \mu\text{m}$, $\lambda_{R\text{eff}} = 0.690 \mu\text{m}$, $\lambda_{I\text{eff}} = 0.830 \mu\text{m}$). Standard stars for null polarization and for the zero point of the polarization position angle were observed several times each night for calibration purposes. Each observation in each filter was corrected for sky polarization and calibrated in the angle in the equatorial system with the proper correction obtained by the data of the angle standards. No correction was done by intrinsic polarization because it was found to be insignificant in the observations of null polarization stars. For further information on the instrument, data acquisition, and data reduction, see Scaltriti (1994).

The polarimetric observations are listed in Table 1, which shows, in self explanatory format, the stellar identification as given by CL, the polarization percentage average (P_λ), and the position angle of the electric vector (θ_λ) through each filter, along with their respective mean errors computed as described by Maronna et al. (1992). Since the Torino photopolarimeter collects photons simultaneously in all the filters (*UBVRI*), the final data from each filter may be of different quality, especially those in the *U*-band. Therefore, observations with values below 3σ error level were ruled out and are not included in Table 1.

According to the photometric membership criteria from Clariá & Lapasset (1986), 18 of the 31 stars reported in this paper are cluster members, one (#69) being a probable member, and 12 stars, nonmembers.

3. Results

The sky projection of the *V*-band polarization vectors for the observed stars in NGC 5749 are shown in Fig. 1. The dot-dashed line superimposed on the figure is the galactic parallel $b = 4.45$ denoting the close alignment of the polarization vectors with the projection of the Galactic Plane. This indicates that the dust along the line of sight is aligned by a magnetic field also close to the direction of the Galactic Disk. This result means that the dust layer responsible for the observed polarization is located in a rather undisturbed place in our Galaxy.

Figure 2 displays the relation that exists between P_V and θ_V (the different symbols are the member and nonmember stars according to CL). Whereas star #68 is a nonmember, stars 31 and 25 are probably located far away behind the cluster. This figure shows an interesting behavior: stars with larger percent values of polarization have a lower angle than stars with low polarization. Most objects with polarization larger than 1% (and a polarization angle θ lower than 80°) are confirmed member stars (CL), while stars with polarization lower than 1% (and $\theta > 80^\circ$) are mostly nonmembers.

This result may also be displayed by the plotting of the run of the polarization vector \mathbf{P} through its components in the equatorial system (the Stokes parameters Q and U). The plot (Fig. 3) provides useful information on variations in interstellar environments: if the light from individual stars of a region of an open cluster has gone through a common sheet of dust, their representative points will concentrate on a given region in the Q vs. U plot, indicating similar optical characteristics in the polarizing

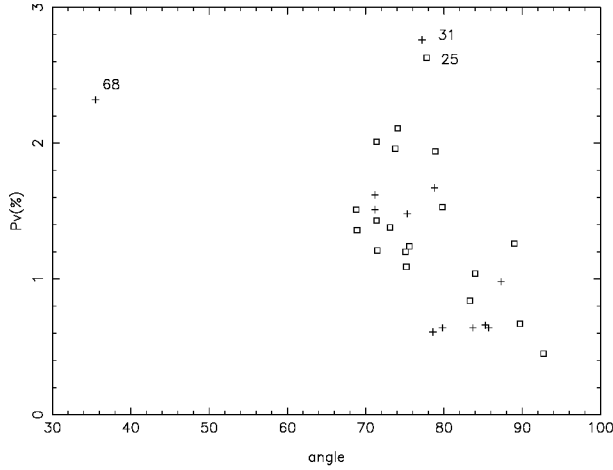


Fig. 2. V-band polarization percentage of the stellar flux $P_V(\%)$ vs. the polarization angle θ_V for each star. Open squares are member stars, while crosses are nonmembers as classified by Clariá & Lapasset (1986).

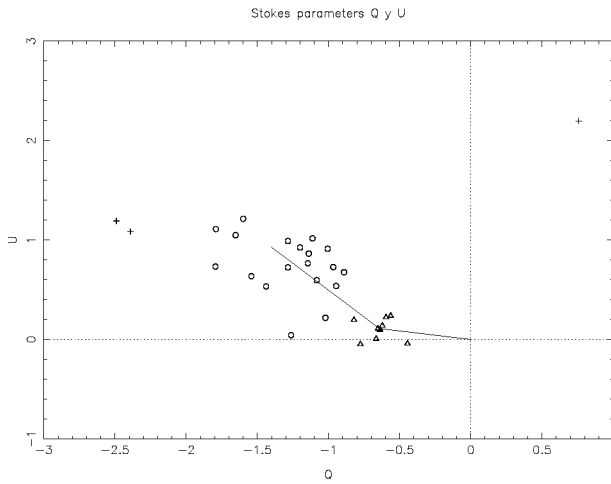


Fig. 3. U vs. Q plot for the stars of NGC 5749. Triangles represent the nearby stars, circles represent the cluster stars and some nonmembers, and crosses stand for the stars behind the cluster.

dust, for both the member and nonmember stars (located behind the dust layer). In the case that a nonmember object is in front of the cloud, this star will not have the same polarimetric properties as those stars located behind the dust cloud. For example, if there are two dust layers, the cluster stars and the nonmember stars behind both clouds will show the same polarimetric properties, but some of the nonmembers stars are likely to be located between both clouds. These stars will show polarimetric characteristics of one cloud only (the one closer to the observer). Therefore, their observations would show different properties than the data from the stars located behind the two dust layers. So, the polarimetric observations could be used as a hard criterion of membership. Also, the combination of both dust layers could lead to an increase in the polarization or in a depolarization depending on the orientation of the dust grains between both dust clouds. This kind of analysis has been successfully applied by Feinstein et al. (2003b), Orsatti et al. (2003), and Martínez et al. (2004) in the polarimetric studies of the open clusters NGC 6231, Pismis 20, Hogg 22, and NGC 6204, respectively.

Figure 3 very clearly shows a close clump of stars #39, 56, 61, 62, 102, 111 with nearly the same parameters Q and U ; also,

near to this group, stars #9, 82, and 104 are found. This group of stars (#39, 56, 61, 62, 102, 111) is so similar in the $Q-U$ space that its weight average is $Q = -0.64 \pm 0.12$, $U = 0.11 \pm 0.2$, ($P = 0.65\%$, $\theta = 84.8^\circ$). If stars #9, 82, and 104 are considered members of this group, the weight average is $Q = -0.63 \pm 0.14$, $U = 0.10 \pm 0.27$ ($P = 0.64\%$, $\theta = 85.5^\circ$). These values are low compared to the other stars observed in the region, and clearly lower than the confirmed cluster members.

It is important to notice that these stars, which have similar polarimetric parameters, are randomly located over the cluster (see Fig. 1); for example, star #111 (HD129896) is the most northwestern observed object, #56 is at the north, stars #39, #82 are close to the core, and star #9 is the most southeastern observed star. This spatial distribution shows that the cloud producing this polarization covers the whole cluster. By the use of the photometry of CL, and the Q parameter (Schmidt-Kaler 1982), the distance for these stars ranges from 300 pcs (#31 and #61) to 700 pcs for #39 (HD 130244) and #102. So, the first cloud, on the light of sight, is at least at 300 pc.

Therefore, we interpreted this clump of stars in the $Q-U$ diagram as a clear indication of a local dust cloud (located in the sun neighborhood) for the following reason: most of these stars are randomly distributed over the cluster; they have some spread in distance (lower than the cluster) and most of them are considered nonmembers by CL (star #56 was classified by CL as a member). The other stars have larger polarization values, so, they are behind another dust cloud.

In Fig. 3, the line running from the origin of the coordinates ($Q = 0, U = 0$, which represents the dustless solar neighborhood) to any other point would indicate the direction of the polarizing vector $P = \sqrt{Q^2 + U^2}$ as seen from the sun. This figure clearly illustrates our interpretation: the observed stars over the region segregate into groups, the nearby nonmembers, nonmembers with polarization values close to the cluster, members of the cluster, and stars behind the cluster. The solid lines represent the changing direction of the vector P connecting the mean (Q, U) values for the groups. A change in direction of vector P can be seen between the nonmember and the member stars, indicating different polarimetric characteristics in the dust causing the polarization. The first group, located near a point representing the solar neighborhood, has low polarization (less than 1%) and the polarization vector direction given by $\theta_v = 84^\circ$. This polarization is produced by a nearby dust cloud. The other group is composed of stars that are mostly accepted as cluster members (CL), and characterized by higher values of polarization (above 1%) and a lower angle ($\theta < 80^\circ$). We also observed a slight change in the direction of vector P inside the cluster, probably due to an intracluster dust component.

3.1. Cluster membership

We analyzed the membership of our 31 star sample based on the polarimetric data collected. The nearby clump of stars previously discussed includes 6 stars (#39, 61, 62, 82, 102, 111) considered nonmembers and 3 that are considered members (#9, 56, 104) by CL. Yet, the low polarization of these last 3 stars provides evidence for claiming that such stars are probably nonmembers. Unless there is some depolarization effect by another polarization component (e.g. intrinsic to the star), they are not located behind the same dust layers as the cluster stars are. The membership of these stars is more thoroughly analyzed in the next section.

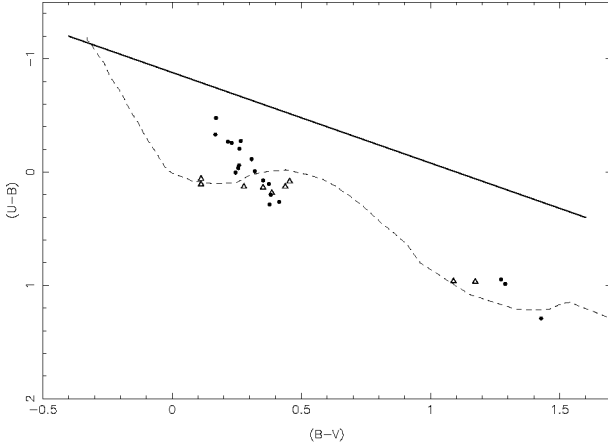


Fig. 4. Remake of the color-color diagram for the cluster. Circles are stars that we now considered as members, while triangles are stars considered nonmembers because of the polarimetric observations. The dashed line is the unreddened main sequence and the full line is the reddening line. The polarization criteria proved very efficient for cleaning the main sequence of field stars.

The cluster itself can be described with the following polarimetric parameters, $P > 1\%$ and $\theta < 80^\circ$. The objects selected with these criteria consist of 19 stars, 15 of which are considered members (#13, 15, 22, 23, 26, 38, 40, 63, 69, 70, 72, 75, 77, 92, 107), and 4 are considered nonmember stars (#28, 46, 93, 110) by CL. The last 4 stars have similar polarization values to the member stars; according to the photometric data (CL) these objects are evolved red stars located between 900 and 1000 pcs from the Sun. Consequently, these stars are probably close, in the line of sight, to the cluster suffering the same extinction; however, they are nonmember field stars. Therefore, this group comprises cluster stars and stars located near the cluster. This interpretation may be also checked by plotting the color-color diagram (Fig. 4) using CL's data, but displaying the stars according to our polarimetric classification in the two groups: the low polarization group and the cluster stars. The plot displays a sharper main sequence and shows that stars #9, 56, and 104, are very probably field stars, so these objects are nonmembers.

In Figs. 2 and 3 there are three stars that do not belong to the cluster or to the group of nearby stars – namely, stars #25, 31, and 68 (considered nonmembers by CL). The last two stars (#31 and 68) have high polarization values (2.76% and 2.32%, respectively), but in this case they can be interpreted as two stars located behind the cluster. In particular, for star #68, if we calculate the Q parameter (Schmidt-Kaler 1982), with the color index $(B - V)$ and $(U - B)$ from the data of CL, we obtain a B8III spectral type. Based on this, the star is located close to 2270 pc, with an $E_{(B-V)} = 0.68$. However, the polarization angle ($\theta_V = 35.5^\circ$, see Table 1) is different if compared to the values of the other stars. This can be the result of the multi-layered composition of dust with different orientations along the line of sight. In the next section this particular star will be discussed in larger detail. As far as star #31 is concerned, it is a nonmember red star (CL).

According to its polarization angle, star #25 belongs to the cluster group and it is a member star (CL), though it has high polarization (2.7%) compared to the values of the other members, and its polarization value and angle are similar to those of star #31. However, this star is a red nonmember, located behind the cluster. Both stars (#25 and #31) are very closely projected in the sky plane (see Fig. 1) and are probably polarized by the same intracluster dust layer. All these examples show how

polarimetry can be used to test cluster membership, particularly in those cases in which field stars have colors similar to those of the cluster members. In the case of NGC 5749, a polarimetric criterion to determine membership renders an excellent result.

4. Analysis and discussion

To analyze the data, the polarimetric observations in the five filters were fitted in each star using Serkowski's law of interstellar polarization (Serkowski 1973). That is:

$$P_\lambda / P_{\lambda_{\max}} = e^{-K \ln^2(\lambda_{\max} / \lambda)}. \quad (1)$$

We assume that, if polarization is produced by aligned interstellar normal dust particles, then the observed data (in terms of wavelength, $UBVRI$) will follow Eq. (1) and each star will have $P_{\lambda_{\max}}$ and λ_{\max} values.

To perform the fitting we adopted $K = 1.66\lambda_{\max} + 0.01$ (Whittet et al. 1992). For each star we also computed the σ_1 parameter (the unit weight error of the fit) in order to quantify the departure of our data from the “theoretical curve” of Serkowski's law. In our scheme, when a star shows $\sigma_1 > 1.5$, it is indicating the presence of intrinsic stellar polarization. The λ_{\max} values can be used to test the origin of the polarization. In fact, those objects having λ_{\max} lower than the average value of the interstellar medium (0.545 μm , Serkowski et al. 1975) are candidates to have an intrinsic component of polarization as well (cf. Orsatti et al. 1998). Another criterion to detect intrinsic stellar polarization involves computing the dispersion of the position angle for each star normalized by the average of the position angle errors ($\bar{\epsilon}$). The values obtained for $P_{\lambda_{\max}}$, the σ_1 parameter, λ_{\max} , and $\bar{\epsilon}$ together with the identification of stars are listed in Table 2.

According to the values of the σ_1 parameter, which estimates how suitable Serkowski's law is when fitted to the observations, we can see that the data of NGC 5749 is well fitted (see Table 2). In all cases, the value of σ_1 is smaller than 1.5 for the confirmed members of the cluster. Only three stars (#13, 63, 75) are likely to have an intrinsic component of polarization; their data shows a rotation on the angles in four filters for star #13 ($BVRI$) and in three filters for star #63 (VRI). Besides, both stars have low polarization, this probably being an indicator that the light of these stars is being depolarized because of the combination of the intrinsic component and the dust component with different angles of the polarization vectors. In particular, the presence of intrinsic polarization in the light from star #75 causes a mismatch between observations and Serkowski's curve fit. Star #62 displays a large σ_1 and $\bar{\epsilon}$, but these values can be the result of the larger error involved in observations of that star. We suspect star #104 has an intrinsic polarization component because of the low polarization in all the filters, the fact that value of the B filter is larger than the V , and given that there is some dispersion of the angles of the data in all the different filters. But on the other hand the observations of this star are close to the 3σ level.

The polarization efficiency of the dust towards NGC 5749 is estimated from the $P_{\lambda_{\max}}$ vs. E_{B-V} individual plots. Individual color excesses E_{B-V} for the member stars are from CL. For some nonmember stars (as classified by CL), the E_{B-V} was estimated from the photometry by calculating the Q parameter (Schmidt-Kaler 1982). For example, star #92 has a high excess (0.46 mag, CL), and this value does not agree with its low polarization (1.3%). But, according to its location in the C-C diagram there are two solutions. Taking into account that the star #92 is a member of the cluster (CL), the adequate solution would be that it belongs to an earlier spectral type (A0-1V). For this spectral

Table 2. Parameters of the Serkowski fit to the linear polarization data for stars in NGC 5749.

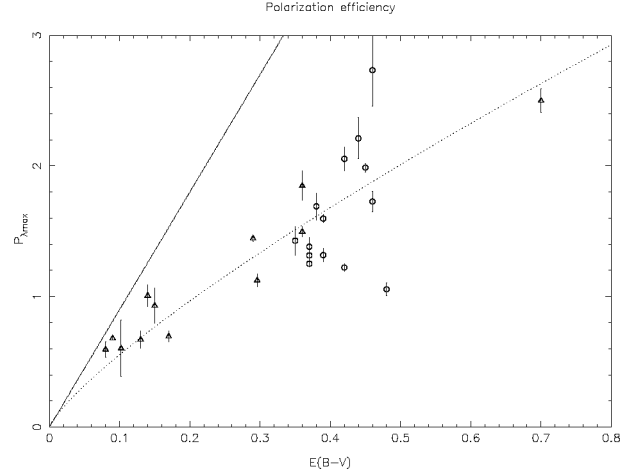
| Stellar identification | $P_{\max} \pm \epsilon_P$ % | σ_1 | $\lambda_{\max} \pm \epsilon_{\lambda_{\max}}$ m μ | $\bar{\epsilon}$ |
|---------------------------|--------------------------------|------------|---|------------------|
| 9 | 1.007 ± 0.084 | 0.702 | 0.600 ± 0.124 | 0.82 |
| 13 | 1.055 ± 0.051 | 0.321 | 0.668 ± 0.071 | 1.72 |
| 15 | 2.212 ± 0.158 | 0.478 | 0.773 ± 0.062 | 2.83 |
| 22 | 1.987 ± 0.032 | 0.220 | 0.605 ± 0.020 | 0.21 |
| 23 | 2.054 ± 0.034 | 0.206 | 0.549 ± 0.017 | 1.33 |
| 25 | 2.734 ± 0.277 | 0.694 | 0.803 ± 0.080 | 0.91 |
| 26 | 1.317 ± 0.053 | 0.850 | 0.637 ± 0.048 | 0.95 |
| 28 | 1.848 ± 0.113 | 0.322 | 0.856 ± 0.072 | 1.33 |
| 31 | 2.824 ± 0.013 | 0.075 | 0.602 ± 0.007 | 0.70 |
| 38 | 1.690 ± 0.103 | 0.614 | 0.703 ± 0.056 | 1.44 |
| 39 | 0.669 ± 0.065 | 0.637 | 0.415 ± 0.054 | 0.65 |
| 40 | 1.098 ± 0.025 | 0.388 | 0.604 ± 0.032 | 0.54 |
| 46 | 1.497 ± 0.038 | 0.264 | 0.670 ± 0.036 | 2.82 |
| 56 | 0.595 ± 0.058 | 0.739 | 0.487 ± 0.099 | 1.20 |
| 61 | 0.680 ± 0.007 | 0.089 | 0.596 ± 0.020 | 3.26 |
| 62 | 0.589 ± 0.183 | 1.905 | 0.679 ± 0.660 | 3.36 |
| 63 | 1.222 ± 0.030 | 0.135 | 0.625 ± 0.051 | 7.57 |
| 68 | 2.499 ± 0.092 | 1.069 | 0.574 ± 0.056 | 0.30 |
| 69 | 1.381 ± 0.069 | 0.405 | 0.630 ± 0.069 | 0.24 |
| 70 | 1.597 ± 0.032 | 0.292 | 0.689 ± 0.021 | 0.92 |
| 72 | 1.427 ± 0.110 | 1.095 | 0.680 ± 0.077 | 1.69 |
| 75 | 1.728 ± 0.080 | 0.555 | 0.503 ± 0.055 | 0.82 |
| 77 | 2.054 ± 0.090 | 0.919 | 0.646 ± 0.043 | 0.64 |
| 82 | 0.930 ± 0.136 | 1.092 | 0.459 ± 0.148 | 2.89 |
| 92 | 1.315 ± 0.036 | 0.309 | 0.502 ± 0.034 | 1.04 |
| 93 | 1.445 ± 0.023 | 0.195 | 0.572 ± 0.024 | 1.60 |
| 102 | 0.695 ± 0.043 | 0.470 | 0.577 ± 0.083 | 0.50 |
| 104 | 0.603 ± 0.217 | 1.375 | 0.698 ± 0.495 | 0.81 |
| 107 | 1.124 ± 0.047 | 0.383 | 0.594 ± 0.047 | 0.10 |
| 110 | 1.668 ± 0.052 | 0.636 | 0.636 ± 0.053 | 0.03 |
| 111 | 0.735 ± 0.059 | 0.754 | 0.621 ± 0.119 | 0.08 |

type, the excess E_{B-V} would be between 0.37–0.40 mag, so the star probably belongs to a less reddened group.

Figure 5 displays $P_{\lambda_{\max}}$ vs. E_{B-V} ; the member and nonmember stars have been plotted using different symbols. Assuming normal interstellar material characterized by $R = 3.2$, the empirical upper limit relation for the polarization efficiency given by $P_{\lambda_{\max}} = R A_v \sim 9E_{B-V}$ (Serkowski et al. 1975). This relation is plotted and indeed, this line represents the maximum efficiency of polarization produced by the interstellar dust. Likewise, the line for $P(\%) = 3.5E_{(B-V)}^{0.8}$, also shown in Fig. 5, represents a new estimate of the average efficiency made by Fosalba et al. (2002). This plot (Fig. 5) shows that there is a group of objects with $E_{B-V} < 0.2$. These stars are #9, 39, 56, 61, 82, 102, and 104, which further confirms that this clump of nearby stars, as clearly show by our polarimetric analysis, is a group of nonmember stars.

In the particular case of the open cluster NGC 5749, the figure indicates that the polarization efficiency appears to be consistent with the average value observed in our Galaxy (Fosalba et al. 2002). But it also shows some scattering in E_{B-V} correlated with $P_{\lambda_{\max}}$. One possible explanation for this scattering in polarization and color excess could be that a dust layer is located inside the cluster, as suggested in Fig. 3.

There is some other evidence of a dust cloud within NGC 5749 because CL have argued that the full width of their C-C diagram for stars with spectral type earlier than about A0V is 0.13 mag. This value exceeds the lower limit of 0.11 mag estimates by Burki (1975) for clusters with differential reddening.

**Fig. 5.** Plot $P_{\lambda_{\max}}$ vs. E_{B-V} for stars of NGC 5749. The solid line is $P_{\lambda_{\max}} = 9E_{B-V}$, and the dotted line is $P_{\lambda_{\max}} = 3.5E_{(B-V)}^{0.8}$. Circles are stars considered members, whereas triangles are stars considered non-members.

Therefore, they conclude that the reddening across the cluster is variable. Figure 5 also shows that the observed member stars split into two groups; one, with a range in color excess of 0.35–0.39 and an average polarization of 1.4%, and the other, more reddened, with a range in excess of approximately 0.42–0.48 mag, but its average polarization is of 2%, excluding stars #13, 63 and 69. We have excluded these stars from the statistics because they are likely to have an intrinsic component of polarization that explains their low polarizations. Hence, this first stellar group inside the cluster is probably composed of “front-side” stars not suffering the internal extinction. So, the E_{B-V} of this group is representative of a dust component located between the field stars and the cluster. Also, as shown in the previous section, star #25 (a member) and star #31 (a nonmember star located behind the cluster) have the same high polarization, and both stars are very close in projection on the sky. Therefore, these objects are polarized by the same dust cloud, which is probably located inside the cluster.

Star #68, located at 2270 pc, has an $E_{B-V} = 0.68$ and the polarization value is slightly lower than the value predicted by Fosalba et al. (2002). Besides, its polarization angle ($\approx 35^\circ.5$), very different from the cluster and from star #31 (which is also a background star), shows that there is a dust layer producing polarization with a different angle in comparison to the one produced by dust in front of NGC 5749 and star #31. Moreover, the final orientation of the polarimetric vector of star #68 is the composition of several dust layers; at least two of them had been identified in this work with the magnetic field in the direction of the Galactic plane, and a component behind the cluster in a very different direction. The resulting polarimetric vector is now in the direction of $\theta = 35^\circ.5$.

5. Summary

The analysis of the polarimetric measures in five bands of 31 stars in the region of the open cluster NGC 5749 shows members and nonmembers with different polarimetric properties. In the nonmember group, some objects seem to be nearby stars, but others are close to the cluster. This result has led to the conclusion that the light from the cluster stars is affected by several dust clouds on its way to the Sun. First, we have a dust component located as far as 300 pc from the Sun, behind this layer, the nearby field stars display a polarization of $P_V = 0.65\%$, with an

angle of $\theta = 83^\circ$, while the other component is lying between these stars and the cluster. This second dust component is responsible for approximately 1% of the total polarization of the cluster ($P_V = 1.7\%$ and the angle $\theta = 74^\circ$). Therefore, both dust layers are producing polarization with a difference in angle of approximately 10° , showing a slight change in the orientation of the magnetic field in front of and behind the nearby field stars.

The polarization efficiency of NGC 5749 is consistent with the observed average in our galaxy. In this region, we have been able to polarimetrically identify an intra-cluster dust component, noticeable in the observations of some member stars as well as of some nonmember stars located behind the cluster (#25 and 31). The presence of dust inside the cluster causes scattering in the E_{B-V} and in the measured polarization percentage; besides, it causes a slight change in the direction of the polarization vector, which is observed in the stars behind the cluster.

The different polarization data of star #68, located far away behind the cluster (approximately 2270 pc), shows that there is a dust layer producing polarization with a different angle (35.5°) compared with the dust cloud in front of NGC 5749. The final orientation of the polarimetric vector of star #68 is the result of the composition of several dust layers, some of them with the magnetic field close to the direction of the Galactic Plane and others behind the cluster, with a different orientation. Once again, polarization has proved to be a good criterion for determining and confirming the membership of the stars of a cluster. In this study, polarimetric data confirmed the membership of twelve (12) stars of the cluster and changed the membership data of six (6) stars.

Acknowledgements. We wish to acknowledge the technical support at CASLEO during the observing runs. We also acknowledge the use of the Torino Photopolarimeter built at Osservatorio Astronomico di Torino (Italy) and operated under agreement between Complejo Astronómico El Leoncito and Osservatorio Astronomico di Torino.

References

- Axon, D. J., & Ellis, R. S. 1976, MNRAS, 177, 499
- Burki, G. 1975, A&A, 43, 37
- Clariá, J. J., & Lapasset, E. 1986, AJ, 91, 326
- Clariá, J. J., & Lapasset, E. 1992, Acta Astron., 42, 343
- Feinstein, C., Baume, G., Vergne, M. M., & Vázquez, R. 2003a, A&A, 409, 933
- Feinstein, C., Martínez, R., Vergne, M. M., Baume, G., & Vázquez, R. 2003b, ApJ, 598, 349
- Fosalba, P., Lazarian, A., Prunet, S., & Tauber, J. A. 2002, ApJ, 564, 762
- Goodman, A. A., Bastien, P., Myers, P. C., & Menard, F. 1990, ApJ, 359, 363
- Lyngå, G. 1964a, Meddn. Lund Astr. Obs., Ser., 2, 139
- Lyngå, G. 1964b, Meddn. Lund Astr. Obs., Ser., 2, 140
- Martínez, R., Vergne, M., & Feinstein, C. 2004, A&A, 419, 965
- Maronna, R., Feinstein, C., & Clocchiatti, A. 1992, A&A, 260, 525
- Mathewson, D. S., & Ford, V. L. 1970, MemRAS, 74, 139
- Orsatti, A.M., Vega, E., & Marraco, H. G. 1998, AJ, 116, 226
- Orsatti, A.M., Vega, E., & Marraco, H. G. 2003, A&A, 408, 135
- Scaltriti, F. 1994, Technical Publication No. TP-001, Osservatorio Astronomico di Torino
- Schmidt-Kaler, Th. 1982, Landolt-Borstein, Numerical Data and Functional Relationships in Science and Technology New Series, Group VI, Vol. 2, ed. K. Schaifers, & H. H. Voigt (Berlin: Springer-Verlag)
- Serkowski, K. 1973, in Interstellar Dust and Related Topics, ed. J. M. Greenberg, & H. C. van de Hulst (Dordrecht: Reidel), IAU Symp. 52, 145
- Serkowski, K., Mathewson, D. L., & Ford, V. L. 1975, ApJ, 196, 261
- Whittet, D. C. B., Martin, P. G., Hough, J. H., et al. 1992, ApJ, 386, 562